JMEPEG
https://doi.org/10.1007/s11665-022-07717-0

1059-9495/$19.00

TECHNICAL ARTICLE

Influence of Post-heat Treatment on Friction Stir-Processed AA7075/SiC Surface Composite Properties

D.S. Chandra Mouli, R. Umamaheswara Rao, A. Raveendra, P. Saritha, and G. Parthasarathi

Submitted: 5 June 2022 / Revised: 2 November 2022 / Accepted: 11 November 2022

The effect of post-aging treatment on the evolution of microstructure and the properties of silicon carbide-reinforced AA7075 surface composite manufactured by friction stir processing (FSP) were explored in this study. For this purpose, FSPed surface composites were subjected to aging treatment at 150, 180, and 210 °C for 8 and 16-h duration. The microstructure and properties such as microhardness and wear resistance were evaluated after aging treatment. The results showed that the grain refinement and homogenous distribution of SiC in matrix together with the precipitation strengthening enhanced the properties of FSPed surface composites. Hardness was found to be decreased at higher aging temperature and duration, due to the abnormal grain growth and the formation of stable precipitated particles in the microstructure. Surface composite samples age-treated to 180 °C for 8 h, and 150 °C for 16 h have exhibited good wear resistance and frictional characteristics. This study demonstrated that the FSP process combined with aging treatment had a significant influence on the microhardness and wear resistance of AA7075/SiC surface composite.

Keywords AA7075/SiC surface composite, Aging treatment, Friction stir processing, Microstructure, Microhardness, Wear resistance

1. Introduction

The most widely used structural materials are aluminum alloys because of their excellent properties. Among aluminum alloys, AA7075 alloy is preferred in aerospace and automobile industries owing to its high-strength-to-weight ratio (Ref 1-3). It is also sensitive to aging heat treatment; therefore, it can be strengthened by the precipitation hardening mechanism (Ref 4). However, they exhibit poor surface characteristics which restricted their use in several tribological applications (Ref 5). In the past few years, many research attempts have been made for improving surface properties of aluminum alloys, and they suggest processes like reinforcing the surface with hard particles and grain refinement methods. Among the various grain refinement methods mentioned in the literature, friction stir processing (FSP) gained popularity, as it can be effectively used to improve the surface characteristics of aluminum alloys by refining grain by dynamic recrystallization mechanism (Ref 6-8). It has been demonstrated that the surface properties of FSPed aluminum alloys can also be enhanced by reinforcing the microstructure with ceramic particles like aluminum oxide and silicon carbide (Ref 9, 10).

The post-heat treatment process has been performed by many investigators to further improve the mechanical properties of the aluminum alloy after FSP (Ref 11-13). Enhancement in the properties was ascribed to grain boundary hardening and precipitate hardening mechanisms (Ref 14). It has been reported that the post-aging process after FSPed aluminum alloy increased the hardness due to the existence of metastable precipitates and their pinning effect at the grain boundaries (Ref 15-17). The number of metastable precipitates was found to increase with the increase in the aging duration which was accountable for the increase in strength (Ref 18).

Recent researches have proposed the possibility of combining the effect of reinforcement and heat treatment such as annealing and artificial aging for improving the properties of the surface composite produced by the FSP process (Ref 19-27). The improvement in the properties such as hardness, wear resistance, and thermal stability of post-heat-treated FSPed aluminum surface composite was achieved due to the combined effect of inhibition of grain growth, the existence of reinforcement particles and the formation of fine precipitates in the microstructure. Owing to the advantages of post-heat treatment after FSP, a detailed study is required to explore the effect of post-heat treatment on the properties of FSPed aluminum alloy surface composite. Thus far, no research work has been performed to investigate the effect of post-aging treatment on the properties of FSPed AA7570/SiC surface composite. In our previous work (Ref 28), the microhardness and the wear resistance of AA7570 alloy were enhanced by incorporating SiC particles on the surface by the FSP process and successfully optimized the processed parameter. The present study focuses mainly to study the outcome of post-aging heat treatment on the mechanical and tribological properties of the FSPed AA7570/SiC surface

D.S. Chandra Mouli, Department of Mechanical Engineering, JNTUK, Kakinada, Andhra Pradesh 533005, India; and Department of Mechanical Engineering, MREC(A), Hyderabad, Telangana 500100, India; **R. Umamaheswara Rao**, Department of Mechanical Engineering, CEC, Visakhapatnam, Andhra Pradesh 530048, India; **A. Raveendra**, Department of Mechanical Engineering, MREC(A), Hyderabad, Telangana 500100, India; and **P. Saritha** and **G. Parthasarathi**, Department of Mechanical Engineering, Anurag University, Hyderabad 500088, India. Contact e-mail: dkmouli1986@gmail.com.

Published online: 09 December 2022

composite. Post-aging treatment was performed with different temperatures and durations, and their effects were systemically analyzed by examining microstructure evolution, microhardness, and wear resistance of the surface composite.

2. Experimental Procedure

In this study, rolled plates of age-hardenable AA7075-T651 alloy having dimensions of 150 × 50 × 6 mm were selected as the base metal. Silicon carbide (SiC) particles with an average size of 37 μm and a density of 3.21 g/cm3 were selected as reinforcing material. SiC particle was preferred as reinforcement owing to its superior mechanical properties, corrosion resistance, low density, and good thermal stability and proved to improve the properties of aluminum and its alloy (Ref 29-31).

Blind holes of size 2 mm with a depth of 3.5 mm were drilled and arranged in an array of 2 × 2 mm for placing the SiC particles. A spacing of 4 mm was provided between the holes, for the uniform distribution of reinforcing particles. Along the work piece length of 150 mm, 50 such holes are made. An automatic vertical milling machine (HMT Ltd. Pinjore, India) with suitable alteration was used in the fabrication of AA7075/SiC surface composites. A flat shoulder FSP tool with a square pin made of an H13 steel tool was used. The shoulder diameter and the length of the tool were 20 and 100 mm, respectively. The size and height of the square pin were 6 and 6 mm, respectively. The photograph and the schematic drawing of the tool are shown in Fig. 1. A pinless tool made of H13 steel was used for the capping process had a diameter and length of 20 and 100 mm, respectively. For concealing the SiC particles in the drilled hole and preventing them from scattering while FSP, the capping process was performed with a rotational speed of 560 rpm, a traverse speed of 25 mm/min, and a plunging depth of 0.3 mm.

After the capping process, AA7075/SiC surface composites were made with a single-pass FSP with the rotational speed, traverse speed, and tilt angle of 1125 rpm, 50 mm/min, and 3°, respectively. These parameters were chosen based on the previous study by authors (Ref 28) that optimized these parameters for enhancing the tribological properties of AA7075/SiC surface composites. During FSP, 8 KN of axial load and 15 s of initial dwelling period were maintained. To avoid the defects like tunneling and voids in the stir zone (Ref 32), FSP was performed with 0.24 mm shoulder penetration depth. Through this process, surface composite with 10% (vol%) SiC was produced. Calculation of volume percentage of reinforcement is provided in Appendix A. After the FSP process, six samples of the surface composite were subjected to the artificial aging process. As the solidus temperature of AA7075 is 477 °C, artificial aging was performed below this temperature. According to the literature (Ref 17), the artificial aging of FSPed surface composite specimen was done. First, the specimen was heated to an elevated temperature and maintained at that temperature for the specified aging time for the formation of the precipitate particles. After the aging time, the specimen was cooled to room temperature in the air. The aging temperatures and time durations selected in this study are presented in Table 1. After the aging process, the samples were cooled to room temperature inside the furnace.

Microhardness was measured with a neighboring indentation distance of 0.5 mm along the transverse section of each surface composite sample using the Vickers microhardness tester (VH-IMDX). Specimens with dimensions of 10 × 10 × 6 mm were used for microhardness test. Hardness measurement was taken according to ASTM E-384 with a load of 500 g and a dwelling time of 20 s. At each location, hardness was measured three times and the average value was considered for hardness data. The wear test was conducted on specimens having dimensions 25 × 5 × 6 mm according to ASTM-G99 using the pin-on-disc tester (DUCOM). The wear test was conducted for 300 s at room temperature in dry conditions. A disc made of hardened chromium steel was used as a counterface. The track diameter of 120 mm, a sliding speed of 175 rpm, and a normal load of 30 N were used during the wear test. The specimens used for microhardness and wear test were machined from the surface composite using wire EDM process. To examine the microstructure and to observe the SiC

Table 1 Artificial aging process schedule for AA7075/SiC surface composite

Sample designation	Temperature, °C	Time, Hrs
150/8	150°	8
150/16	150°	16
180/8	180°	8
180/16	180°	16
210/8	210°	8
210/16	210°	18

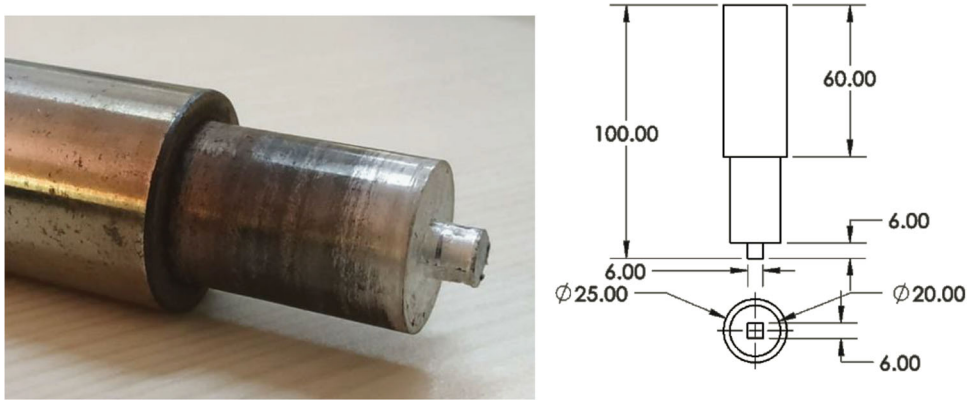

Fig. 1 Photograph and the dimension of FSP tool (all dimensions are in mm)

distribution on the stir zone surface, a scanning electron microscope (JSM-6330) with built-in energy-dispersive spectroscopy (EDS) was used.

3. Results and Discussion

3.1 Microstructure

Figure 2 presents the microstructure at the stir zone surface of the FSP samples after artificial aging treatment at different temperatures and times. Homogeneous distribution of SiC particles without any traces of agglomeration was observed in the matrix of all the FSP samples. Interestingly, ring-shaped white spots were noticed in the microstructure. These white rings were found to increase with the increase in aging temperature and time. They were analyzed by EDS, and the spectrum and the element composition are presented in Fig. 3. EDS result indicated the formation of precipitates. During the early phase of the artificial aging process, the precipitates of $MgZn_2$ formed along the grain boundaries help to prevent the dislocation movement and thereby improve the strength of the 7075 aluminum alloy by precipitation strengthening mechanism (Ref 4, 15, 33, 34). When the aging temperature and time are increased further, these precipitates grow in size and get increased in volume fraction, thus enhancing the precipitation strengthening.As seen in Fig. 3, when the alloy over-aged at a temperature of more than 180 °C, these precipitates are incoherent with the matrix material and they became ineffective in resisting the dislocation movement. This leads to the reduction in the strength of the 7075 aluminum alloy (Ref 12, 18, 35).

3.2 Microhardness

The effect of aging treatment on the microhardness at base metal, thermomechanically affected zone (TMAZ), heat-affected zone (HAZ), and stir zone (SZ) of artificially aged samples in comparison with the non-aged FSP sample is pictorially shown in Fig. 4. In all the cases, microhardness was found to be lesser in the base metal, whereas it was increased gradually from HAZ and reached a high value at the stir zone. The lower hardness at HAZ and TMAZ is attributed to the grain growth that occurred during FSP. The maximum hardness of 125 Hv was obtained at the stir zone when the aging treatment was performed at 180 °C for 8 h.

The microhardness profile of the FSP samples after the artificial aging process conducted at various temperatures for 8 and 16 h is shown in Fig. 5(a) and (b), respectively. These figures show that the values of hardness across the transverse section of the FSP samples vary depending on the selected artificial aging temperature and duration. The microhardness profiles of all the samples showed a general increase in hardness at the stir zone when compared to the other zones. The fine grains formed owing to dynamic recrystallization and the presence of uniformly distributed SiC particles are responsible for the increase in hardness at the stir zone. At 8-h aging duration (Fig. 5a), as the aging temperature increased, hardness increased initially up to 180 °C and then decreased. For 16 h of aging duration (Fig. 5b), the hardness at the stir zone tends to decrease with the increase in aging temperatures considered in this study. At the higher aging duration, the hardness increases by the formation of fine precipitates as explained earlier. At higher aging temperature and duration, hardness decreased because of the occurrence of over aging. Over-aging normally occurs for AA7075 alloy beyond 180 °C. Hence at 180 °C, microhardness reached the highest value. Beyond 180 °C (i.e., 210 °C), over-aging occurred which resulted in abnormal grain growth and an increase in the precipitated particles (Ref 11, 36). It was reported elsewhere (Ref 12) that increase in aging time and temperature results in over-aging, which caused the decrease in hardness. As the aging time increases, the precipitation formation becomes more prevalent, resulting in

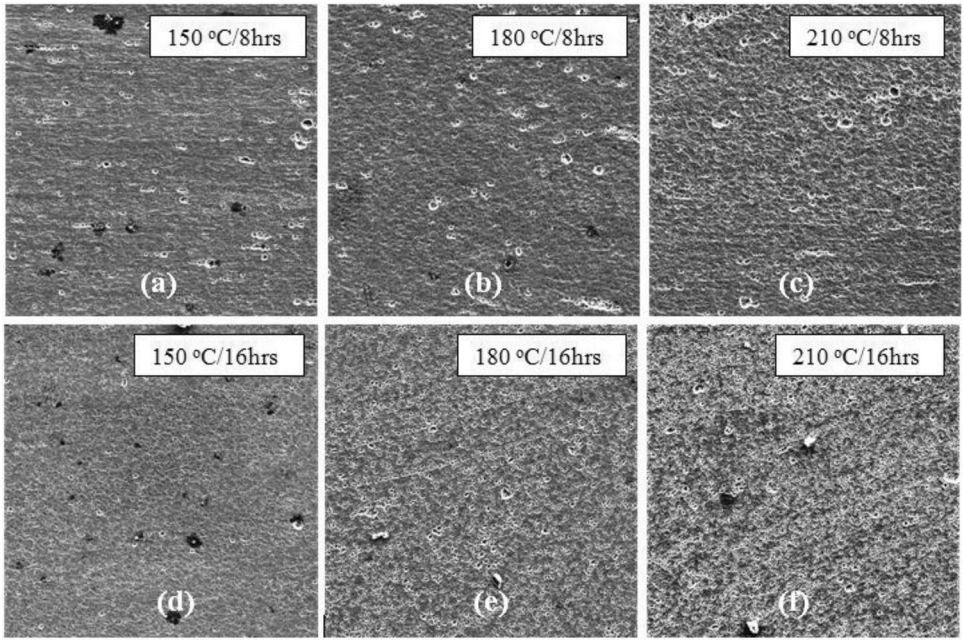

Fig. 2 Surface microstructure of stir zone of the FSP samples obtained at different aging temperatures and times (magnification: 500X, Scale: 100 μm)

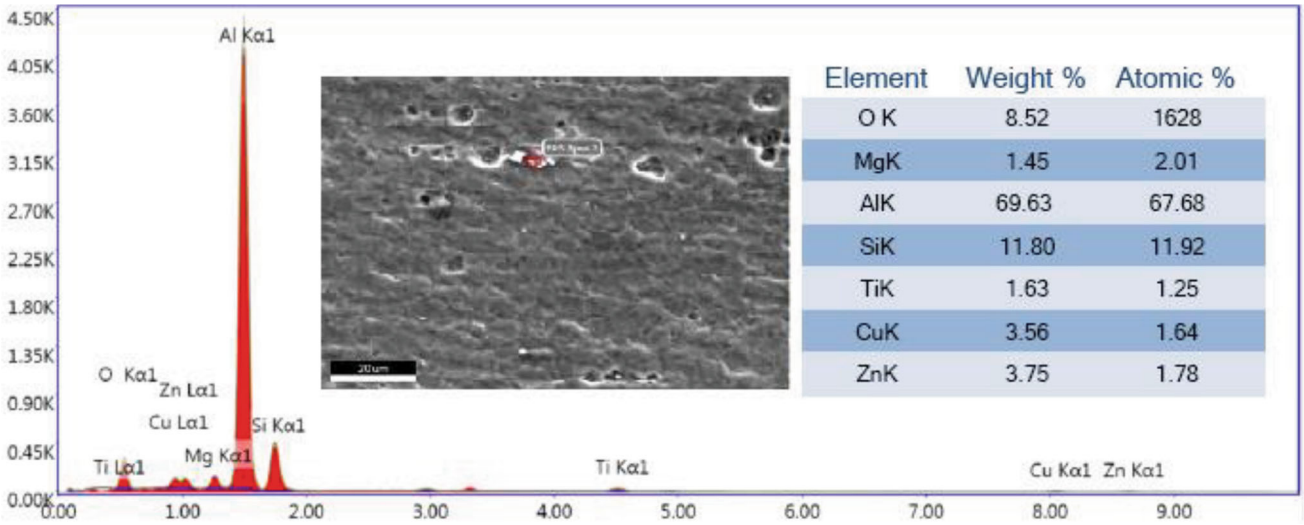

Fig. 3 Result of the EDS analysis on 210/8 FSP specimen showing the spectrum and the elemental composition

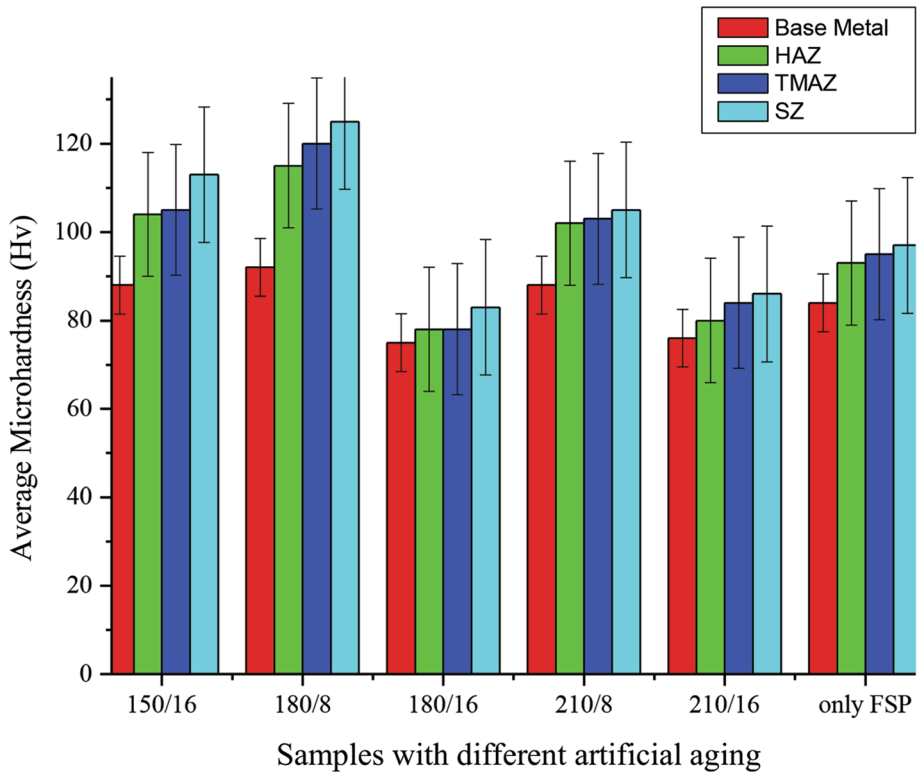

Fig. 4 Average microhardness at different zones of the aged and non-aged FSP samples

the hardness reduction of the aluminum alloy. Even though reinforcing particles are present in the microstructure, due to high aging temperature they could not effectively increase pinning force for restricting the grain growth (Ref 37).

4. Wear Characteristics

Figure 6(a) and (b) presents the variation of specific wear rate with time for different FSP samples aged at 8 and 16 h, respectively.

From Fig. 6 (a) and (b), it was evident that the specific wear rate of all the age-treated FSP samples gradually increased as the time duration of the wear test increased. Among the age-treated FSP samples, samples aged to 180 °C for 8 h and 150 °C for 16 h have exhibited lower wear rate. These two samples had higher microhardness because of the reasons explained earlier. The hardened surface of the samples permitted less plastic deformation due to the SiC reinforcement, grain refinement, and the formation of hard precipitates in the matrix. All these phenomena resulted in lower wear rate. However, as the time duration of the wear test increased, there was a frictional heat generation at the interface which caused the

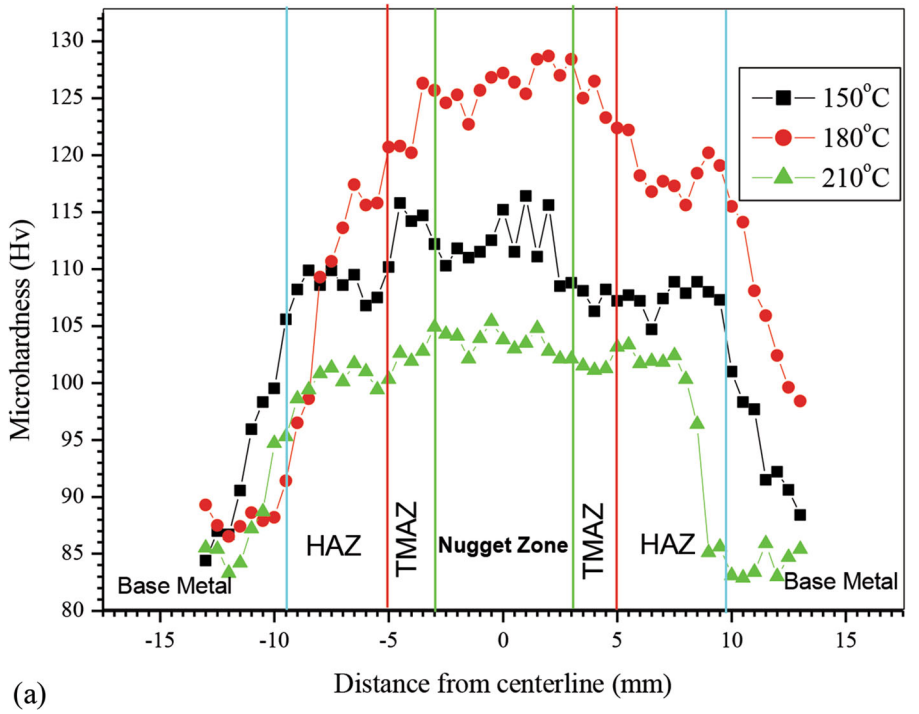

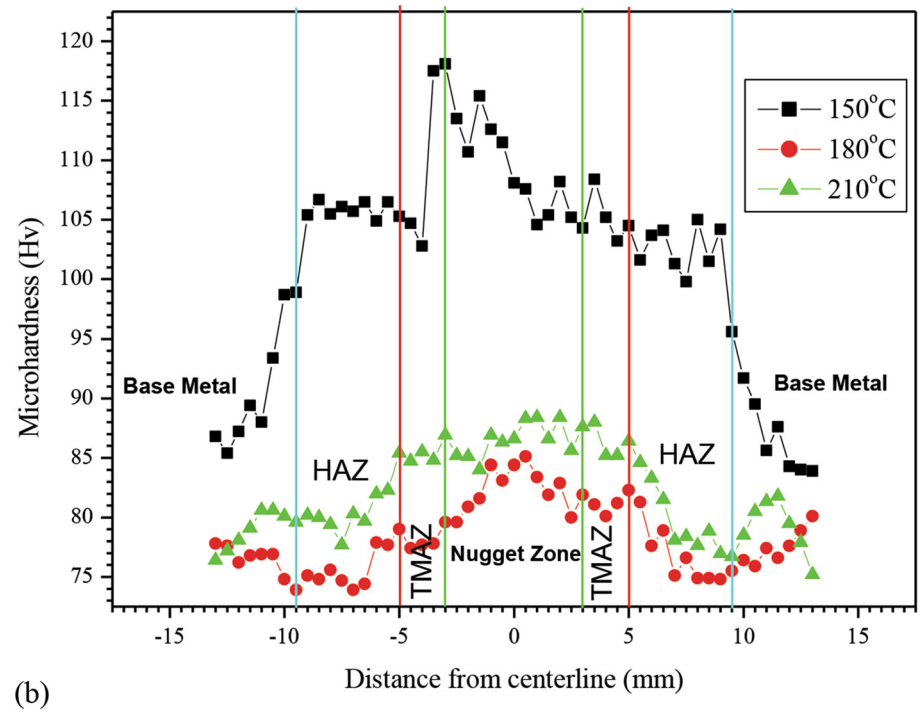

Fig. 5 Variation of the microhardness of FSP samples at different aging temperatures for (a) 8 h and (b) 16 h

thermal softening of the surface. As a consequence of this, there was an increase in wear rate with time.

Figure 7(a) and (b) represents the variation of friction coefficient with sliding time of the age-treated FSP samples for 8 and 16 h, respectively, under sliding wear test. The average coefficient of friction at each temperature for 8 and 16 h is presented in Table 2. The coefficient of friction was found to be fluctuating over the entire time duration of the test for all the FSP samples. These fluctuations may have resulted from the variation of contact surface area between FSP samples and the disc counterface of the wear tester due to the presence of SiC reinforcement and the precipitates in the matrix. From Fig. 7(a) and (b) and Table 2, it was clear that samples with high microhardness, namely 180/8 and 150/16, have shown lower wear rate and coefficient of friction. Hence, it can be concluded that these samples have good wear resistance and frictional characteristics.

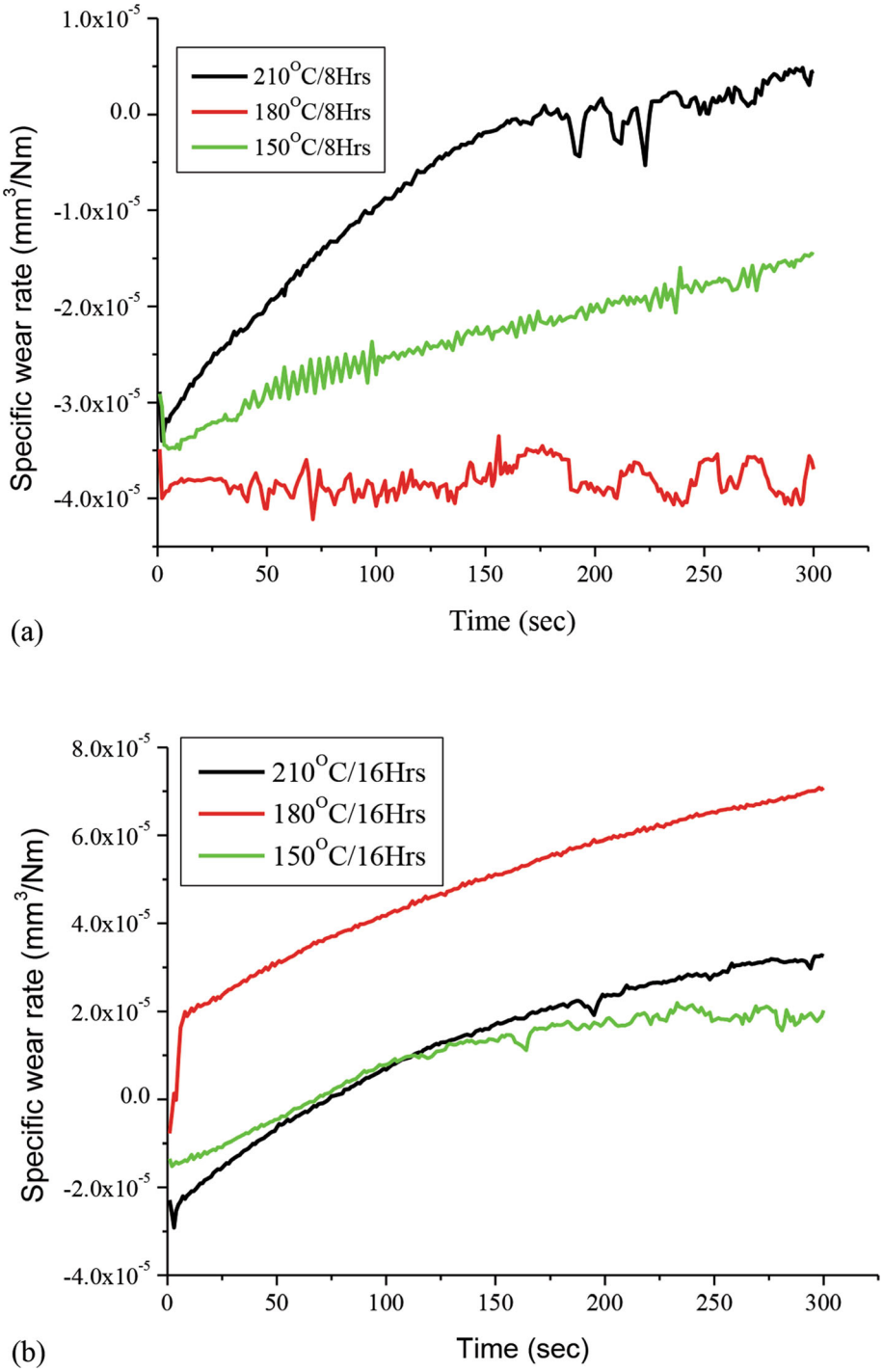

Fig. 6 Variation of specific wear rate with time of the FSP samples aged at different temperatures for (a) 8 h and (b) 16 h

5. Conclusions

The effect of post-aging heat treatment on the mechanical and tribological properties of the FSPed Al7570/Sic surface composite was studied in this research work. The influence of temperature and duration of the aging process were analyzed by examining microstructure, microhardness, and specific wear rate of the surface composite. The research findings are as follows:

1. Homogeneous distribution of SiC particles was observed in the microstructure of all the FSP samples without any traces of agglomeration.
2. EDS analysis revealed that the artificial aging process performed after FSP formed $MgZn_2$ precipitate along the grain boundary.
3. The microhardness and wear resistance of AA7075/SiC surface composite are improved by the particle strengthening and precipitation strengthening mechanisms.

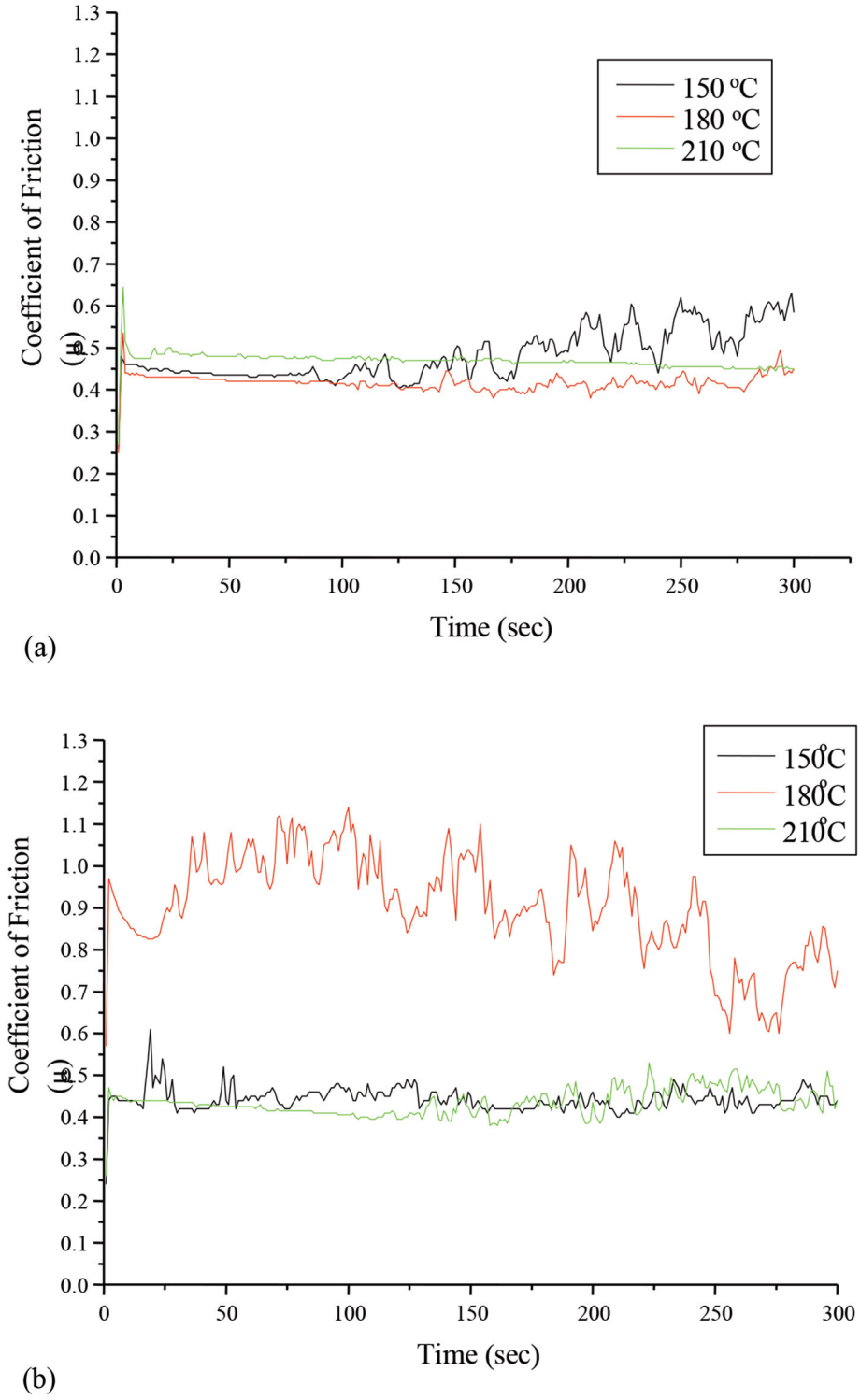

Fig. 7 Variation of coefficient of friction for (a) 8 h and (b) 16 h of age treatment

4. At 8 h of aging, hardness increases up to 180 °C due to the formation of fine precipitates.
5. At higher aging temperature and duration, hardness decreased because of the abnormal grain growth and the formation of stable precipitated particles in the microstructure.
6. FSPed AA7075/SiC surface composite samples age-treated to 180 °C for 8 h and 150 °C for 16 h have exhibited good wear resistance and frictional characteristics. This is attributed to the SiC reinforcement, grain refinement, and the formation of hard precipitates in the matrix.

Table 2 Average coefficient of friction at different aging temperatures and times

Aging temperature, °C	Aging time	
	8 h	16 h
150	0.48	0.42
180	0.44	0.90
210	0.47	0.43

Appendix

Volume fraction of reinforcement in FSP can be easily calculated by taking the volume of the base metal on which FSP is to be performed (without holes) as the total volume. Then, the volume fraction of reinforcement can be calculated as the sum of the volume of holes divided by total volume. In this research work, blind holes of size 2 mm were drilled arranged in an array of 2 × 2 mm with a depth of 3.5 mm. Fifty such holes are made along the work piece length of 150 mm. Total volume of all holes are 549.78 mm^3. Volume of the base metal on which FSP was done is 150 × 6 × 6 mm = 5400 mm^3. Hence, the volume percentage of the reinforcement is calculated as follows:

$$\begin{aligned}&\text{Volume percentage of the reinforcement}\\&= (\text{Total volume of holes}/\text{Volume of the base metal on which FSP was done}) \times 100\\&= (549.78/5400) \times 100\\&= 10.18\%\,(\text{Approx. as } 10\%)\end{aligned}$$

References

1. Y.D. Zhang, S.B. Jin, P.W. Trimby, X.Z. Liao, M.Y. Murashkin, R.Z. Valiev, J.Z. Liu, J.M. Cairney, S.P. Ringer, and G. Sha, Dynamic Precipitation, Segregation and Strengthening of an Al–Zn–Mg–Cu Alloy (AA7075) Processed by High-Pressure Torsion, *Acta Mater.*, 2019, **162**, p 19–32.
2. S.K. Patel, V.P. Singh, B.S. Roy, and B. Kuriachen, Recent Research Progresses in Al-7075 based In-situ Surface Composite Fabrication Through Friction Stir Processing: A Review, *Mater. Sci. Eng., B*, 2020, **1**(262), 114708
3. A.T. Guner, D. Dispinar, and E. Tan, Microstructural and Mechanical Evolution of Semisolid 7075 Al Alloy Produced by SIMA Process at Various Heat Treatment Parameters, *Arab. J. Sci. Eng.*, 2019, **44**(2), p 1243–1253.
4. O.Z. Gokhan and A. Karaaslan, Properties of AA7075 Aluminum Alloy in Aging and Retrogression and Reaging Process, *Trans. Nonferrous Met. Soc. China.*, 2017, **27**(11), p 2357–2362.
5. A. Baradeswaran and P.A. Elaya, Effect of Graphite on Tribological and Mechanical Properties of AA7075 Composites, *Tribol. Trans.*, 2015, **58**, p 1–6.
6. V. Sharma, U. Prakash, and B.M. Kumar, Surface Composites by Friction Stir Processing: A Review, *J. Mater. Process. Technol.*, 2015, **224**, p 117–134.
7. V. Sudhakar, G. Madhu, K.M. Reddy, and R. Srinivasa, Enhancement of Wear and Ballistic Resistance of Armour Grade AA7075 Aluminium Alloy using Friction Stir Processing, *Def. Technol.*, 2015, **11**, p 10–17.
8. V.V. Patel, V. Badheka, and A. Kumar, Friction Stir Processing as a Novel Technique to Achieve Superplasticity in Aluminum Alloys: Process Variables, Variants, and Applications, *Metallogr. Microstruct. Anal.*, 2016, **5**(4), p 278–293.
9. N. Pol, G. Verma, R.P. Pandey, and T. Shanmugasundaram, Fabrication of AA7005/TiB2-B4C Surface Composite by Friction Stir Processing: Evaluation of Ballistic Behavior, *Def. Technol*, 2018, **15**, p 1–6.
10. H. Rana and V. Badheka, Elucidation of the Role of Rotation Speed and Stirring Direction on AA 7075–B4C Surface Composites Formulated by Friction Stir Processing, *Proc. Inst. Mech. Eng. Part L J. Mater. Des. Appl.*, 2019, **233**(5), p 977–994.
11. Y.F. Hou, C.Y. Liu, B. Zhang, L.L. Wei, H.T. Dai, and Z.Y. Ma, Mechanical Properties and Corrosion Resistance of the Fine Grain Structure of Al–Zn–Mg–Sc Alloys Fabricated by Friction Stir Processing and Post-Heat Treatment, *Mater. Sci. Eng., A*, 2020, **21**(785), 139393
12. S. Kilic, I. Kacar, M. Sahin, F. Ozturk, and O. Erdem, Effects of Aging Temperature, Time, and Pre-strain on Mechanical Properties of AA7075, *Mater. Res.*, 2019, **12**, p 22.
13. Chauhan K, Satyanarayana MV, Kumar A. Effect of tool geometry and heat treatment on friction stir processing of AA6061. In: Advances in Applied Mechanical Engineering 2020 (pp. 947–953). Springer, Singapore
14. X.H. Zeng, P. Xue, L.H. Wu, D.R. Ni, B.L. Xiao, and Z.Y. Ma, Achieving an Ultra-High Strength in a Low Alloyed Al Alloy Via a Special Structural Design, *Mater. Sci. Eng. A*, 2019, **755**, p 28–36.
15. S. Gholami, E. Emadoddin, M. Tajally, and E. Borhani, Friction Stir Processing of 7075 Al Alloy and Subsequent Aging Treatment, *Trans. Nonferrous Met. Soc. China*, 2015, **25**(9), p 2847–2855.
16. Y.F. Hou, J.J. Xiao, C.Y. Liu, and B. Zhang, Effect of Heat Treatment on the Microstructure, Mechanical Properties, and Corrosion Resistance of Friction Stir Processed Al-Zn-Mg-Cu-Sc-Zr Alloy, *J. Mater. Eng. Perform.*, 2021, **30**(5), p 3398–3405.
17. P.K. Mandal, R.J. Kumar, and J.M. Varkey, Effect of Artificial Ageing Treatment and Precipitation on Mechanical Properties and Fracture Mechanism of Friction Stir Processed MgZn2 and Al3Sc Phases in Aluminium Alloy, *Mater. Today Proc.*, 2021, **1**(46), p 4982–4987.
18. I. Charit and R.S. Mishra, Effect of Friction Stir Processed Microstructure on Tensile Properties of an Al-Zn-Mg-Sc Alloy Upon Subsequent Aging Heat Treatment, *J. Mater. Sci. Technol.*, 2018, **34**(1), p 214–218.
19. Z. Chen, J. Li, A. Borbely, G. Ji, S.Y. Zhong, Y. Wu, M.L. Wang, and H.W. Wang, The Effects of Nanosized Particles on Microstructural Evolution of an In-situ TiB2/6063Al Composite Produced by Friction Stir Processing, *Mater. Des.*, 2015, **25**(88), p 999–1007.
20. D. Ghanbari, M.K. Asgarani, K. Amini, and F. Gharavi, Influence of Heat Treatment on Mechanical Properties and Microstructure of the Al2024/SiC Composite Produced by Multi–Pass Friction Stir Processing, *Measurement*, 2017, **1**(104), p 151–158.
21. L. Ke, C. Huang, L. Xing, and K. Huang, Al–Ni Intermetallic Composites Produced In situ by Friction Stir Processing, *J. Alloy. Compd.*, 2010, **503**(2), p 494–499.
22. F. Khodabakhshi, A. Simchi, A.H. Kokabi, A.P. Gerlich, and M. Nosko, Effects of Post-annealing on the Microstructure and Mechanical Properties of Friction Stir Processed Al–Mg–TiO2 Nanocomposites, *Mater. Des.*, 2014, **1**(63), p 30–41.
23. M.S. Khorrami, M. Kazeminezhad, and A.H. Kokabi, Thermal Stability of Aluminum After Friction Stir Processing with SiC Nanoparticles, *Mater. Des.*, 2015, **5**(80), p 41–50.
24. I.S. Lee, P.W. Kao, C.P. Chang, and N.J. Ho, Formation of Al–Mo Intermetallic Particle-Strengthened Aluminum Alloys by Friction Stir Processing, *Intermetallics*, 2013, **1**(35), p 9–14.
25. D.R. Ni, J.J. Wang, Z.N. Zhou, and Z.Y. Ma, Fabrication and Mechanical Properties of Bulk NiTip/Al Composites Prepared by Friction Stir Processing, *J. Alloy. Compd.*, 2014, **15**(586), p 368–374.
26. J. Qu, H. Xu, Z. Feng, D.A. Frederick, L. An, and H. Heinrich, Improving the Tribological Characteristics of Aluminum 6061 Alloy by Surface Compositing with Sub-micro-size Ceramic Particles Via Friction Stir Processing, *Wear*, 2011, **271**(9–10), p 1940–1945.
27. J. Mohamadigangaraj, S. Nourouzi, and H.J. Aval, The Effect of Heat Treatment and Cooling Conditions on Friction Stir Processing of A390–10 wt% SiC Aluminium Matrix Composite, *Mater. Chem. Phys.*, 2021, **15**(263), 124423
28. D.S. Mouli and R.U. Rao, Optimization of Friction Stir Process Parameters for Micro-Hardness and Wear Characteristics of Silicon Carbide-Reinforced Al-7075 Surface Composite, *Trans. Indian Inst. Met.*, 2021, **24**, p 1–9.
29. A.P. Reddy, P.V. Krishna, R.N. Rao, and N.V. Murthy, Silicon Carbide Reinforced Aluminium Metal Matrix Nano Composites-A Review, *Mater. Today Proc.*, 2017, **4**(2), p 3959–3971.

30. M.H. Rahman and H.M. Al Rashed, Characterization of Silicon Carbide Reinforced Aluminum Matrix Composites, *Proc. Eng.*, 2014, **1**(90), p 103–109.
31. M.S. Surya and G. Prasanthi, Manufacturing, Microstructural and Mechanical Characterization of Powder Metallurgy Processed Al7075/SiC Metal Matrix Composite, *Mater. Today Proc.*, 2021, **1**(39), p 1175–1179.
32. D.K. Lim, T. Shibayanagi, and A.P. Gerlich, Synthesis of Multi-walled CNT Reinforced Aluminium Alloy Composite via Friction Stir Processing, *Mater. Sci. Eng. A*, 2009, **507**(1–2), p 194–199.
33. M.H. Shaeri, M.T. Salehi, S.H. Seyyedein, M.R. Abutalebi, and J.K. Park, Microstructure and Mechanical Properties of Al-7075 Alloy Processed by Equal Channel Angular Pressing Combined with Aging Treatment, *Mater. Des.*, 2014, **57**, p 250–257.
34. T. Hu, K. Ma, T.D. Topping, J.M. Schoenung, and E.J. Lavernia, Precipitation Phenomena in an Ultrafine-Grained Al Alloy, *Acta Mater.*, 2013, **61**, p 2163–2178.
35. L. Zhang, Y.F. Hou, C.Y. Liu, H.F. Huang, and H.M. Sun, Effects of Short-Time Heat Treatment on Microstructure and Mechanical Properties of 7075 Friction Stir Welded Joint, *J. Mater. Eng. Perform.*, 2021, **19**, p 1–9.
36. J. Chen, L. Zhen, S. Yang, W. Shao, and S. Dai, Investigation of Precipitation Behavior and Related Hardening in AA 7055 Aluminum Alloy, *Mater. Sci. Eng. A*, 2009, **500**(1–2), p 34–42.
37. M.M. Attallah and H.G. Salem, Friction Stir Welding Parameters: a Tool for Controlling Abnormal Grain Growth During Subsequent Heat Treatment, *Mater. Sci. Eng. A*, 2005, **391**, p 51–59.